Tsunami and storm deposits preserved within a ria-type rocky coastal setting (Siracusa, SE Sicily)

G. Scicchitano, B. Costa, A. Di Stefano, S.G. Longhitano and C. Monaco

with 8 figures and 5 tables

Summary. Sedimentological and palaeoecological observations, accompanied by archaeological determinations and absolute dating, have been carried out on a recent beach-barrier system succession located 20 km south of Siracusa, south-eastern Ionian coast of Sicily (Italy). These deposits fill the back edge of a *ria* incised within Miocene limestones and are composed of three main stratal units characterized by distinct sedimentological features. The two lower units, formed by cross-bedded sands and laminated clays, recorded the development of a small confined beach-barrier depositional system, influenced by frequent high-energy events. The upper unit, represented by chaotic coarser sediments, can be attributed to a destructive marine high-energy event. The physical properties of the composing stratal units and the morphological setting of the study area allowed us to reconstruct a suite of storm- and tsunami-related marine depositional processes that might have occurred in recent times along this area of elevated seismicity. In particular, absolute dating and archaeological determinations allow correlating the upper unit to a tsunami wave triggered by the 1693 AD catastrophic earthquake. The same depositional mechanism can also account for some of the coarse levels occurring into the underlying stratal units.

Keywords: Tsunami deposits, storm deposits, coastal morphology, Sicily, Italy

1 *Introduction*

Tsunami waves typically affect coastal areas subject to permanent or frequent current reworking, that are environments characterized by a low preservation potential for "event deposits" (Dawson & Stewart 2007 and references therein). Conversely, beach-barrier systems in the innermost part of narrowing engulfed rocky coasts can be considered as a highly-conservative depositional setting for sedimentary deposits triggered to destructive high-energy marine events. In these conditions, tsunami deposits can be sufficiently preserved by marine erosion or alluvial sediment covering and, when exposed, their interpretative analysis can be considered as a high-potential tool for interpreting anomalous marine events occurred in the past.

Eastern Sicily is one of the most seismically active areas of the central Mediterranean. Normal faulting accommodates WNW-ESE oriented extension, active along the Siculo-Calabrian rift zone (Fig. 1a; Monaco & Tortorici 2000). In eastern Sicily the normal fault belt is mostly located offshore and is marked by a high level of crustal seismicity (Postpischl 1985; Boschi et al. 1995) that generated several tsunamis along the Ionian coast of south-eastern Sicily in historical times (Soloviev et al. 2000; Tinti et al. 2004). The effects of the 1169 AD, 1693 AD and 1908 AD tsunamis are still recognizable in the Siracusa coastal area where boulders up to 182 tons in weight, encrusted by dated marine organisms, were removed and transported inland at a distance of up to 70 m (Scicchitano et al. 2007). Tsunami deposits can be recorded also in other different coastal settings along the same area, where sediment deposited after high-energy events can be sufficiently preserved by the erosive action of incident waves and by other depositional alluvial processes. An impressive example of this condition is represented by the narrow embayment of Ognina, located about 20 km south of Siracusa (Fig. 1b). In the innermost part of this engulfed area, sediments of distinct features have been paid of attention and a sedimentological and paleoecological analysis, accompanied by archaeological determinations and absolute dating, has been carried out in order to determine their possible correlation with depositional mechanisms of tsunami waves.

The analysis and discussion of the physical attributes detected within the Ognina sediments suggest that the morphological setting of the rocky coast in which the deposits were preserved, played a fundamental role for the hydraulic amplification of anomalous marine events and their consequent depositional processes within supratidal coastal environments. Detailed field analyses and discussion on the sediment properties allowed us to reconstruct distinct coastal depositional processes and suggested an interpretative model for the emplacement of the whole sedimentary sequence.

2 *Tectonic setting*

South-eastern Sicily (Fig. 1a) constitutes the emerged foreland of the Siculo-Maghrebian thrust belt and it is characterized by a continental crust overlain by thick Mesozoic to Quaternary carbonate and terrigenous sequences, and volcanics mainly outcropping in the Hyblean Plateau (A.A.V.V. 1987). The Ionian sector of the Hyblean Plateau is located on the footwall of a large normal fault system which since the Middle Pleistocene (Bianca et al. 1999) has reactivated the Malta Escarpment, a Mesozoic boundary separating the continental domain from the oceanic crust of the Ionian basin (Scandone et al. 1981; Makris et al. 1986; Sartori et al. 1991; Argnani & Bonazzi 2005).

Active faulting contributes to a continuous extensional deformation from eastern Sicily to western Calabria (Siculo-Calabrian rift zone, Fig. 1a; Monaco et al. 1997; Monaco & Tortorici 2000). The ESE-WNW extension direction is deduced from structural analysis (Tortorici et al. 1995; Monaco et al. 1997; Jacques et al. 2001; Ferranti et al. 2007), seismological data (Cello et al. 1982; Gasparini et al. 1982; Anderson & Jackson 1987; CMT 1976–2006 and RCMT 1997–2006 Catalogues) and from VLBI (Ward 1994) and GPS (D'Agostino & Selvaggi 2004) velocity fields. In eastern Sicily the normal faults are mostly located offshore, and control the Ionian coast from Messina to the eastern lower slope of Mt. Etna, joining southwards to the system of the Malta Escarpment (Fig. 1a). Offshore fault activity is related to historical seismicity characterized by intensities of up to XI–XII MCS and M ~7, such as the 1169 AD, 1693 AD and 1908 AD events (Baratta 1901; Postpischl 1985; Boschi et al. 1995). Several earthquake-generated tsunamis struck the Ionian coast of south-eastern Sicily in historical times (AD 1169, 1329, 1693, 1818, 1908, 1990; Tinti et al. 2004). According to published geological data and numerical modeling, the seismogenic sources of these events should be located in the Messina Straits and in the Ionian offshore (the Malta Escarpment) between Catania and Siracusa (Monaco & Tortorici 2007 and references therein).

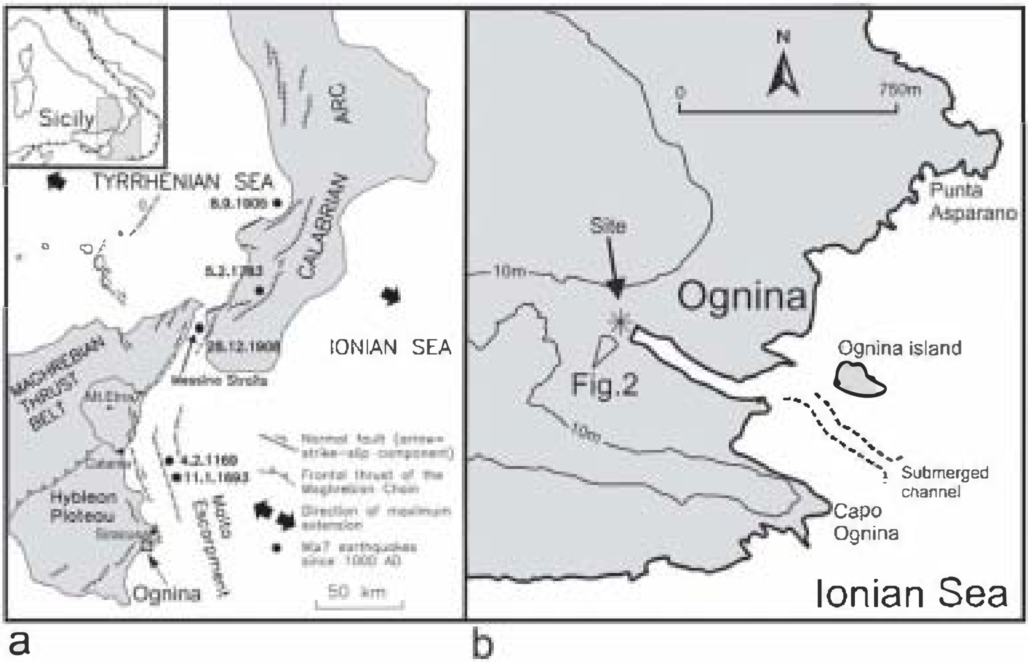

Fig. 1. (a) Seismotectonic sketch map of the Siculo-Calabrian rift zone (SCRZ; Monaco & Tortorici 2000) and its location in the central Mediterranean area (line with triangles indicates the frontal thrust of the orogenic belt). (b) Geographical position of the studied site along the Ionian coast of south-eastern Sicily, in the Siracusa area, see (a) for location.

3 *Sedimentological and paleoecological analysis*

3.1 *Methods*

The present study is based on a detailed facies analysis and lateral correlation of sedimentological logs measured along a study section. Logging has been accompanied by grain size, morphology, sphericity and roundness estimation focused on the pebbly clastic fraction. The outcrop was sketched freehand with the assistance of enlarged coloured photomosaic (Fig. 2) on which the main boundaries were traced, in order to reconstruct spatial variability and geometrical features of the composing lithosomes. Fossil assemblages were determined in micro- (foraminifers) and macro- (molluscs) associations. Samples for foraminiferal analyses were first dehydrated in oven at 40 °C, subsequently disaggregated in distilled water and washed with a 63 µm sieve. Semi-quantitative analyses were performed on all the samples using optical microscope (magnification of 40–100x). Semi-quantitative analyses of molluscs were determined in the > 40 µm fractions. The followed mollusc species nomenclature is after Sabelli et al. (1990) and each species was attributed to a biocenosis according to the bionomic model of Pérès & Picard (1964). Radiocarbon dating of marine organisms and archaeological age determinations on pottery fragments have been performed in order

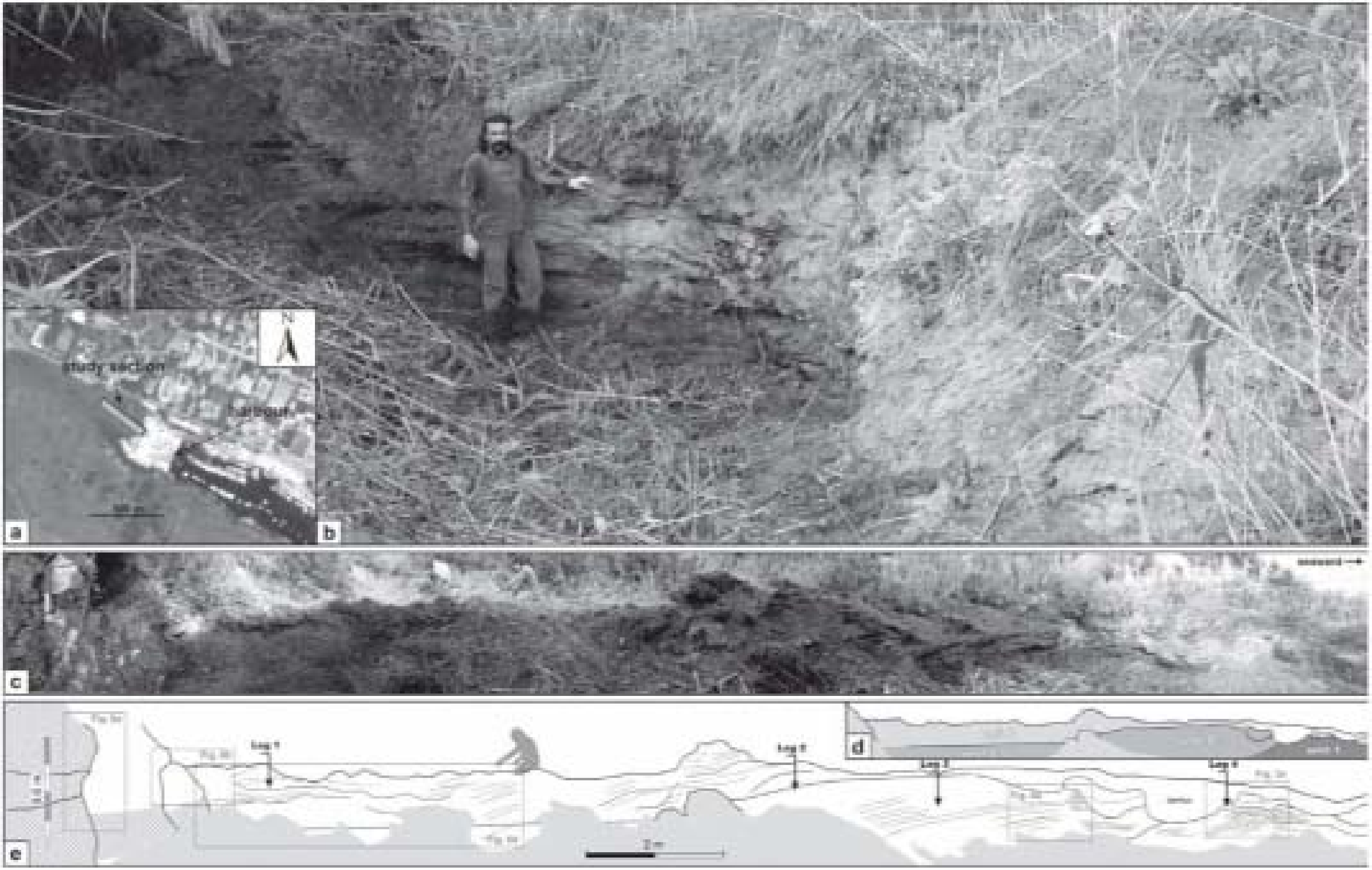

Fig. 2. (a) Aerial photograph showing the location of the study section. (b) Panoramic (inland) view of the section. (c) Photomosaic of the study section (the orientation is WNW-ESE). (d) Outcrop sketch showing the three composing Stratal Units 1, 2 and 3, and (e) the main stratigraphic architectures with log and photo locations.

to constrain the deposition timing of the recognized stratal units and to reconstruct the depositional evolution of the area. All age determinations are AMS ^{14}C, analysed at the Poznań Radiocarbon Laboratory (Poland).

3.2 *The Ognina section*

The outcrop is exposed along a natural section located on the edge of a coastal embayment incised within Miocene limestones (Figs. 1b and 2a). Within this *ria*, a fossilized Holocene beach-barrier system lying unconformably onto the Miocene calcareous bedrock, has been preserved by marine erosion of the dominant waves thanks to the internal and protected position and to the recent construction of a little harbour quay at the end of the natural channel. The Ognina section (Fig. 2c) is ENE-WSW oriented, 20 m long and 0.3–1.8 m thick. It shows a stratigraphic sequence made of fine to coarse grained sediments that can be divided into three stratal units bounded by disconformity surfaces, which have been distinguished through their textural characters and physical attributes (Table 1; Figs. 2d and 2e).

Table 1. Overall morphological, stratigraphic and sedimentary features identified for Stratal Units 1, 2 and 3 composing the Ognina section.

Features	Stratal Unit 1	Stratal Unit 2	Stratal Unit 3
morphological	- the unit thins inland and occupies the outermost (seaward) segment of the section; overall geometry impossible to outline because the top is truncated;	- the unit is confined in the central segment of the section; the overall geometry is tabular;	- the unit occupies the entire section, has a wedge-shaped geometry and thickens landward;
stratigraphic	- the base, not visible in outcrop, is supposed to be gradational on to the bedrock or pre-existing beach deposits; the top is truncated; - the unit is organized into two cross-stratified sub-units *1a* and *1b* forming a landward- and a seaward-dipping foreset, respectively;	- the base is gradational on to the Stratal Unit 1 and is sharp on to the calcareous bedrock; - the unit is organized into two superimposed sub-units *2a* and *2b*;	- the base is erosive and cuts the underlying Units 1 and 2; the top is a surface of modern exposure. - the outermost part of the unit is massive, whilst the innermost part consists of two landward-dipping clinobedded sub-units *3a* and *3b*;
sedimentary	- very well sorted mixed (siliciclastic/bioclastic) sands and granules, organized into foreset lamination; - cross-lamination indicates traction and sand avalanching over a long-term period of deposition.	- sub-unit *2a* is erosive-based and contains fining-upward lenses of shell fragments, pebbles and bioclastic granules passing to cross-laminated silts and flat-laminated clays; these lenses suggest overwash deposition from high-energy waves; - sub-unit *2b* is gradational-based and consists of thinner horizons of very well sorted sands passing to clays with flat- lamination, organized into cm-scale rhythmic cycles; this interval suggests deposition in a low-energy protected area.	- very unsorted sands, granules and gravels apparently massive to indistinctly organized; - clinobedded sub-units consist of erosive based, inverse graded beds of chaotic sub-angular to rounded clasts; - neptunian dikes and calcareous breccias occur at the interface between the innermost part of the unit and the bedrock.

3.2.1 *Stratal Unit 1*

The lowermost Stratal Unit 1 (Table 1; Figs. 2d and 3) is confined in the easternmost (seaward) sector of the section and consists of alternating sandy and gravelly layers of varying thickness containing small shell fragments and pebbles. Sediments are very well sorted though they are organized in packages of laminae of different grain size, ranging from medium to very coarse sands to granules. Finer fraction is totally absent. This unit is cross-stratified and can be furthermore divided into two foreset sub-units, showing opposite directions of migration. The lower sub-unit (1a in Fig. 3a) represents a cross-bed up to 0.8 m thick, characterized by angular foreset inclined up to 25°. Foreset lamination shows a landward direction of migration and is formed by alternating coarser and finer mixed siliciclastic/bioclastic particles (Fig. 3b). Part of it exclusively consists of laminated small-sized molluscs and gastropods (Fig. 3c), whereas small pebbles (up to 5 cm) sparsely occur within the unit. The upper sub-unit (1b in Fig. 3a), 20–25 cm thick, consists of finer particles (medium sands with scattered small pebbles) organized in low-angle (up to 10°), seaward-dipping foreset lamination (Fig. 3a). The top is represented by an irregular erosive surface overlain by the Stratal Unit 3. Organic content (Table 2) is represented by abundant molluscs, benthic foraminifers and fragments of echinoids (*Paracentrotus lividus*), and subordinate bryozoans. Mollusc content (samples A and B in Table 3) is characterised by mostly encrusted and broken shells. Abundant specimens of species belonging to the biocenosis of *Posidonia* meadows (HP) and photophilic algae (AP), such as the gastropods *Gibbula ardens*, *Jujubinus exasperatus*, *Rissoa ventricosa* and the bivalve *Venericardia antiquata* are also present. Species with wide ecological distribution (lre) such as *Bittium reticulatum* and *Cerithium vulgatum* occur in high percentage. *Hydrobia ventrosa* and other lagoon species are badly preserved and scarcely present.

Table 2. Organic content of the examined samples. Frequency: R = rare; C = common; A = abundant.

STRATAL UNITS	1		2									3		
SAMPLES	A	B	C	D	E	F	G	H	I	J	K	L	M	N
MOLLUSCS	A	A	C	A	A	C	A	A	A	C	A	A	A	A
FORAMS	A	A	A	A	C	A	A	C	A	A	C	A	A	A
OSTRACODS	R		C	A	C	A		A	C	A	R	R	C	C
ECHINOIDS *(Paracentrotus lividus)*	C	C			A	R	C	C	C	R	A	C	A	A
BRYOZOAN	A	A	C	A	A	C		A	A	A	A	A	A	A
SERPULIDS	C			C	A	R	A	C	A	C	C	C	C	
CRUSTACEA	R			R					R					R
POSIDONIA			A	A		A								
CORALLINE ALGAE				R								R		R
SPICULES			R	R	R	C	R	R	C	R	C		R	R

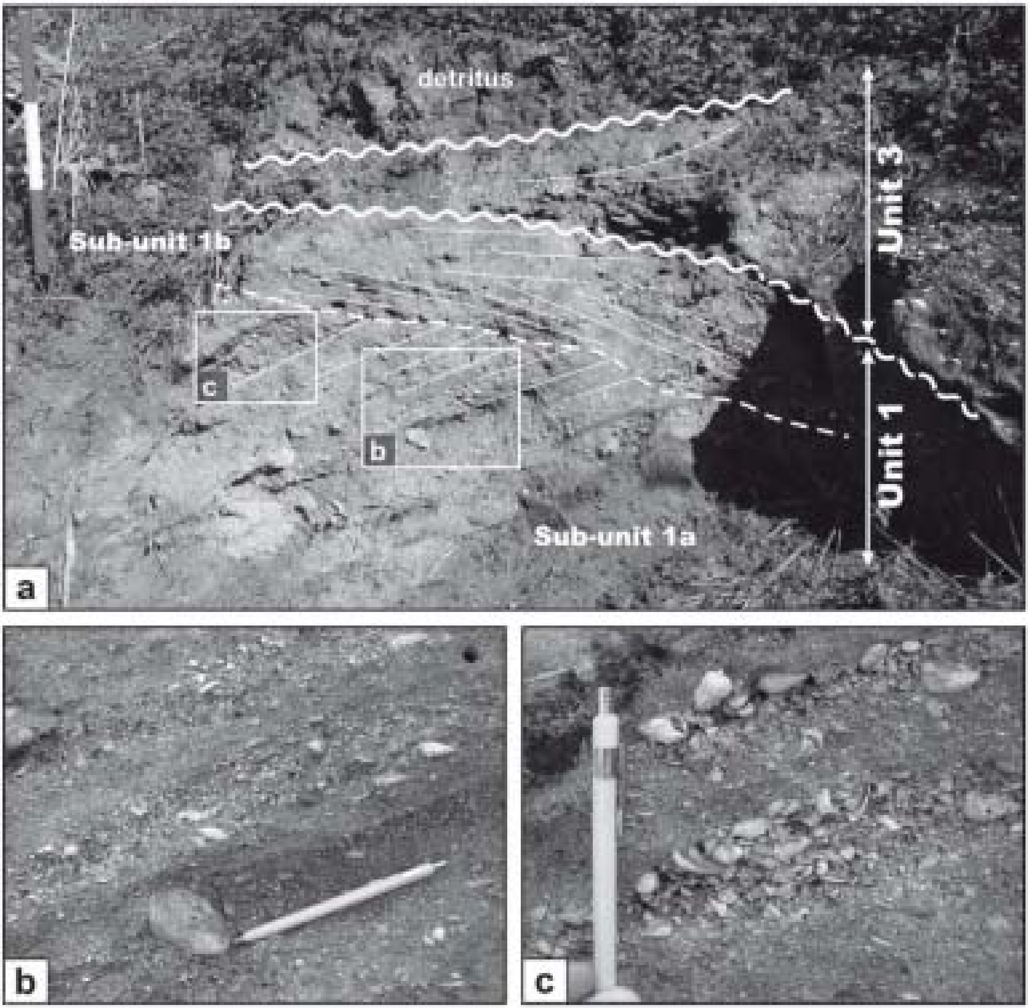

Fig. 3. (a) Outermost outcrop of the Ognina section showing the erosive contact between Stratal Units 1 and 3 (see fig. 2e for location along the study section). In turn, Stratal Unit 1 consists of two sub-units (1a and 1b) exhibiting landward- and seaward-dipping high-angle foresets, respectively. (b) Foreset laminae of sub-unit 1a. Large clasts sparsely occur along the lee face. (c) Detail of sub-unit 1a. Foreset laminae display alternating bioclastic-rich intervals.

3.2.2 *Stratal Unit 2*

The intermediate Stratal Unit 2 (Table 1; Figs. 2d and 4) occupies the central segment of the Ognina section, onlaps both the underlying Unit 1 and the calcareous bedrock and consists of bioclasts-rich sands, silts and clays. The thickness ranges from 0.3 m, where the underlying calcareous bedrock crops out, up to 1.8 m in the depocentre zone. Sediments can be subdivided into two sub-units (Fig. 4a): the lowermost sub-unit 2a is about

Table 3. Bionomic distribution of the mollusc species. Biocenosis nomenclature after Pérès & Picard (1964) and Pérès (1967). LDL = biocenosis of the slowly-drying wracks; RMI = biocenosis of the lower mid-littoral rock; LEE = euryaline and eurythermal biocenosis in brackish waters; SVMC = biocenosis of the superficial muddy sands in sheltered areas; SFBC = biocenosis of fine well-sorted sands; HP = biocenosis of the *Posidonia* meadows; AP = biocenosis of the photophilic algae; SGCF = biocenosis of coarser sands and fine gravel under the influence of bottom currents.

STRATAL UNITS	1		2									3		
SAMPLES	A	B	C	D	E	F	G	H	I	J	K	L	M	N
LDL														
Truncatella subcylindrica	RR			RR	R	RR	RR		R	RR	RR	RR		
Ovatella myosotis					RR		RR							
LEE														
Hydrobia acuta	R						R	RR	C	R	R	RR	RR	R
Hydrobia ventrosa	R	R	C	A	A	R	A	C	A	A	C	R	R	A
Cyclope neritea	R	R			RR	RR	RR	RR	RR			RR	RR	
Cerastoderma glaucum	RR		R	R	C		C	RR	R					
Abra ovata	RR	RR	R	R	R		R	RR	R	RR	RR	RR	RR	RR
SVMC														
Conus mediterraneus	RR	RR			RR		RR		RR		RR		RR	
Loripes lacteus	R	C	RR	R	C		C	RR	R	R	R	R	R	RR
Ctena decussata var.			RR					RR	RR			RR	RR	
Venerupis aurea	RR	RR												
SFBC														
Neverita josephinia											RR			
Acanthocardia tuberculata		R		RR	RR		RR	RR	RR	RR	RR		RR	
Spisula subtruncata													RR	
Chamelea gallina	RR													
AP														
Acmaea virginea							RR		RR					
Tornus subcarinatus										RR				
Gibberulina clandestina	RR	RR							RR			RR	RR	
Mytilaster minimus													RR	
HP														
Gibbula ardens	A	A	RR	RR	R	RR	R	RR	R	RR	R	R	R	RR
Gibbula guttadauri	RR	RR												
Jujubinus exasperatus	A	A			RR	RR	RR	RR	RR	RR	R	R	R	
Alvania beani	RR	RR		RR			R	RR	C	R	C	RR	RR	R
Barleeia unifasciata	RR	RR	RR					RR		R	RR	RR	R	R
Mitrolumma olivoidea												RR		
Venericardia antiquata	C	A			RR		RR	RR	RR	RR	R	RR	R	
AP-HP														
Tricolia pullus	RR	RR			RR		RR	RR	RR		RR			RR
Rissoa auriscalpium											RR			
Rissoa guerinii					RR		RR						RR	
Rissoa variabilis					R		R	RR	RR	RR	RR	R	R	
Rissoa ventricosa	A	A	RR		R		R	R	C	R	A	A	A	
Alvania cancellata		RR												
Alvania cimex					RR		RR				RR	RR	RR	RR
Alvania discors					RR		R	RR			RR	RR		RR
Folinia (Manzonia) costata							RR		RR					
Pusillina radiata					R		R		RR		RR			R
Gibberula miliaria	RR	RR	RR		RR		RR		RR	RR	RR	R	RR	
SGCF														
Calyptraea chinensis										RR				
Goodallia triangularis	RR	RR												RR
Plagiocardium papillosum	RR	RR												

Table 3 (continued). Bionomic distribution of the mollusc species. Biocenosis nomenclature after Pérès & Picard (1964) and Pérès (1967). DC = biocenosis of detritic coastal bottoms; lre = species with wide ecological distribution; sspr = species without a definite ecological significance. Frequency: RR = very rare; R = rare; C = common; A = abundant.

STRATAL UNITS	1		2									3		
SAMPLES	A	B	C	D	E	F	G	H	I	J	K	L	M	N
DC														
Diodora graeca		RR												
Melanella (Eulima) polita							RR						RR	
lre														
Cerithium vulgatum juv.	A	A		R	C	RR	C	R	C	R	C	C	C	C
Bittium reticulatum	A	A			R		R	RR	R		C	C	C	RR
Naticarius millepunctatus	RR	RR												
Nucula nucleus	RR	RR												
sspr														
Crepidula unguiformis								RR						
Euspira sp. juv.				RR					RR	RR				RR
Hinia incrassata	R	RR									RR			
Hinia reticulata		RR			RR	RR								
Mangelia costata											RR			
Raphitoma echinata	RR	RR										RR		
Raphitoma linearis	RR				RR							RR		
Chrysallida indistincta														RR
Turbonilla lactea	RR	RR									RR	RR	RR	RR
Retusa truncatula	RR	RR		RR	RR				RR		RR	RR		RR
Ringicula conformis	RR	RR												
Lepton nitidum	RR	RR		R	R		R	RR	R	R	RR	RR		RR
Parvicardium ovale								RR	RR		RR			

1 m thick and is organized into five (beds nos. 1 to 5 in Fig. 5) fining-upward 10 to 25 cm thick horizons, each characterized by a basal sharp surface and formed by a tripartite pattern of mixed bio-/siliciclastic coarse sand, silt and dark clay intervals. Some of these beds (beds no. 3 and no. 5 in Fig. 5) exhibits a concave erosive basal surface characterized by a concentration of mollusc fragments, small pebbles and bioclastic granules (Fig. 4b). In each level, this interval passes upwards to cross-laminated silt and flat-laminated dark clay. The uppermost sub-unit 2b (Fig. 4a) is about 0.8 m thick and consists of a rhythmic succession of seven (beds nos. 6 to 12 in Fig. 5) horizons, formed by thinner fining-upward 5 to 12 cm thick beds. Compared with the underlying sub-unit, these beds show a lack of erosive surfaces, shell fragments and pebbles basal concentration, but thicker laminated clay intervals (Fig. 4c).

Mollusc assemblages deriving from sub-unit 2a (samples C and D in Table 3) are generally badly preserved, not particularly rich and show low diversity. They are dominated by both adult and juvenile specimens of euryaline and eurythermal lagoons biocenosis species. *Loripes lacteus*, a characteristic species of the superficial muddy sands in sheltered areas biocenosis (SVMC), occurs in low abundance. Species of other biocenotic stocks related to marine infralittoral environment are scarce. *Posidonia* fragments are particularly abundant in sample C, whereas *Paracentrotus lividus* remains are absent (Table 2). Mollusc content of sample E and from samples G to K is more abundant and shows higher diversity.

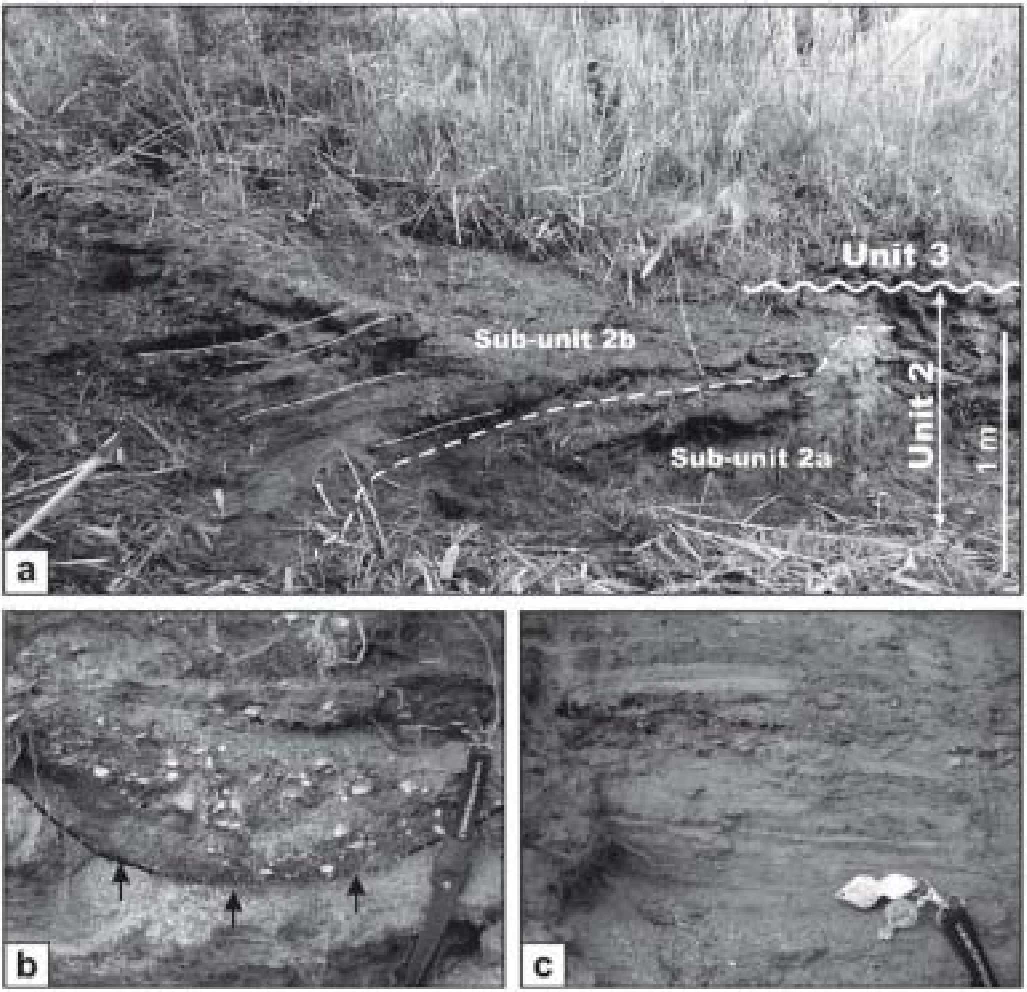

Fig. 4. (a) Erosive contact between Stratal Unit 2 and Stratal Unit 3 cropping out in the central segment of the study section (see fig. 2e for location). Stratal Unit 2 consists of two sub-units (2a and 2b). (b) Detail of sub-unit 2a showing a lens of coarse-grained sediment with erosive base (arrows) and bioclastic fragments concentration. (c) Detail of sub-unit 2b showing flat-laminated silt and clay.

It is represented by a mixture of brackish water and marine benthic species. *Abra ovata, Cerastoderma glaucum, Hydrobia ventrosa*, species belonging to euryaline and eurythermal biocenosis in brackish waters, dominate in the samples collected from the sub-unit 2b. Species of the biocenosis of *Posidonia* meadows (HP) and photophylic algae (AP) are abundant as well. *Cerithium vulgatum* and *Bittium reticulatum*, wide ecological distribution gastropods, are well represented in the assemblage.

The foraminifer content of Stratal Unit 2 is abundant and shows high diversity (Table 4). It consists of typical lagoon species, such as *Ammonia tepida* and smooth carapax ostracods,

Table 4. List of benthic foraminifers yielded in the examined samples. Reworked benthic and planktonic foraminifers are also listed. Frequency: RR = very rare; R = rare; C = common; A = abundant.

	STRATAL UNITS	1		2									3		
	SAMPLES	A	B	C	D	E	F	G	H	I	J	K	L	M	N
BENTHIC FORAMINIFERS	*Adelosina* spp.				R					R			RR		
	Ammonia beccarii	R	R		R					R				R	R
	Ammonia tepida			R	A	C	C	C	A	A	C	C	C	C	C
	Asterigerinata mamilla			RR	RR						RR				
	Astrononion stelligerum				RR	R			R	RR					
	Bolivina sp.						RR		R						
	Calcituba polimorpha					R		R		C		A	R	A	C
	Cibicidella variabilis					R	R		R	RR		R	R		R
	Cibicides refulgens				RR		R			RR	C				R
	Cibicides vermiculatus													R	
	Cribrostomoides jeffersi								RR						
	Discorbis sp.								RR						
	Elphidium advenum														
	Elphidium complanatum			RR	R				R		RR				
	Elphidium crispum	C	C	R	A	A	R	C	A	A	C	C	C	C	C
	Elphidium decipiens														R
	Florilus boueanus					RR									
	Guttulina communis				RR	RR									RR
	Lachanella variolata	RR				R						R			R
	Lobatula lobatula	R		R	A	A	R	C	A	A	A	C	A	C	C
	Massilina secans	R	R			R				R		R	R	C	
	Miniacina miniacea	A	R			R		R		R		C	C	R	C
	Nubecularia lucifuga	A	A	C	R	C	R	A	C	A	R	A	A	A	A
	Peneroplis planatus/P. pertusus	C	R	R		R	R	R	R	C	R	C	C	C	A
	Planorbulina mediterranensis	R			R			R		R		R	R		
	Quinqueloculina spp.	C	R		C	C	C	C	C	C	C	A	C	C	A
	Rosalina bradyi						C			RR	C				
	Rosalina obtusa			R	C	C	C	R	C	C	A	R	R	C	C
	Sorites orbicularis	R	R			R		R	R	C	RR	C	R	C	R
	Sphaerogypsina globula	R	R							R					R
	Spiroloculina spp.	RR		R						R		R		R	
	Textularia spp.				R									R	
	Triloculina spp.	C	R	C				R	C	R		A	R	C	C
	Trochammina inflata				R										
	Vertebralina striata			RR	R				R		RR				
REWORKED BENTHIC FORAMINIFERS	***Amphicorina scalaris***				RR										
	Anomalinoides helicinus					RR					RR				
	Bulimina costata												RR		
	Cassidulina subglobosa			RR	RR					RR		RR	RR	RR	
	Cibicidoides sp.					R				RR					RR
	Lagena striata						RR								
	Lenticulina calcar														RR
	Martinottiella communis							RR							
	Melonis sp.													RR	
	Planulina ariminensis					RR						RR			
	Pullenia bulloides						RR								
	Siphonina planoconvexa				RR										
	Sphaeroidina bulloides						RR								
	***Uvigerina** peregrina*			RR	RR		RR			RR					
	***Uvigerina** rutila*										RR	R			RR
	Frequency	R	R	C	C	C	A	C	C	C	A	R	A	A	C
	Globigerina bulloides	X		X	X	X	X		X	X	X			X	
REWORKED PLANKTONIC FORAMINIFERS	***Globigerina falconensis***							X				X	X	X	
	Globigerinoides elongatus		X	X	X	X	X		X	X	X	X	X	X	X
	***Globigerinoides** extremus*			X		X		X			X		X		
	Globigerinoides obliquus						X		X	X			X	X	
	Globigerinoides ruber											X			
	***Globigerinoides** gr. trilobus*	X		X	X	X	X	X	X	X	X		X	X	X
	Globorotalia aemiliana					X									
	Globorotalia crassaformis												X		
	Globorotalia margaritae					X			X				X		
	Globorotalia puncticulata			X	X		X	X	X	X	X	X	X	X	X
	Globoturborotalita apertura		X		X		X		X				X	X	
	Neogloboquadrina acostaensis					X	X		X	X				X	
	Orbulina universa			X	X	X	X						X		X
	Sphaeroidinellopsis seminulina									X			X		

associated to shallow marine water forms (*Elphidium crispum, E. complanatum, Sorites orbicularis, Triloculina* spp., *Quinqueloculina* spp.) and species preferably living in *Posidonia* meadows (*Lobatula lobatula, Nubecularia lecifuga, Rosalina obtusa*). It is worthy of note the presence of high percentage of reworked planktic species mainly from Upper Miocene and Lower Pliocene horizons, chiefly within the lowermost sub-unit 2a. Sample F is characterized by poor, badly preserved mollusc assemblage and very abundant *Posidonia* fragments. Molluscs are present with few specimens of brackish species (*Hydrobia ventrosa* and *Cyclope neritea*) and very rare species of *Posidonia* meadows biocenosis (*Gibbula ardens, Jujubinus exasperatus*).

Several pottery and glass fragments have been found at distinct levels in the bioclastic lenses. The top of Stratal Unit 2 is characterized by an extensive erosive surface on which the overlying Stratal Unit 3 develops (Fig. 2).

3.2.3 *Stratal Unit 3*

The uppermost Stratal Unit 3 (Table 1; Figs. 2d and 6) corresponds to a widespread wedge of coarse to very coarse sands and granules, containing many pebbles and shell fragments. This body erosively lies over the previous units for the whole section extent, thickening inland from 0.5 to 1 m, and lapping on Miocene limestones (landward termination of the section; Fig. 6a). Sediment displays variable textural characters: i) particle lithology is mainly represented by limestone and calcarenitic clasts, ranging in grain size from medium-fine sand to granule and pebble; rare gneiss and schist pebbles occur; ii) the shape of largest clasts ranges from disks to rods; iii) the sphericity index ranges from low to medium; iv) the roundness index indicates well rounded to angular clasts. Stratal Unit 3 shows an overall inland decreasing of the average grain size and can be divided into two segments that occupy the outer (seaward) and the inner (landward) part of the section, respectively. The outer portion is prevalently unorganized: clasts are randomly floating within a coarse matrix together with mollusc remains to form a single massive bed (Figs. 6b and 6c). The inner portion (Fig. 6d) shows a certain degree of internal organization, represented by gently to high-angle (up to 40°) landward-dipping clinostrata, separated by indistinct, irregular bounding surfaces of erosive truncation. Strata consist of unsorted, reverse-graded clasts (Fig. 6e). This inner portion is composed by two superimposed sub-units (3a and 3b in Fig. 6e). The lowermost sub-unit 3a consists of repeated landward-dipping angular clinostrata, characterized by 1.5–2 m thick foresets directly lapping onto the bedrock. In the upper portion, thinner foresets dipping in the opposite direction (seaward) occur (Fig. 6e). This sub-unit is top truncated by an irregular erosive surface on which the clinostrata of the uppermost sub-unit 3b downlap. This uppermost sub-unit is irregularly cross-stratified and consists of a single landward-dipping, 1–1.2 m thick foreset, made up of reverse graded beds of chaotic sand-rich gravels and scattered sub-angular pebbles (Fig. 6e). The landward contact of the Stratal Unit 3 against the calcareous bedrock is diffusely characterized by several injection structures filling pre-existing fractures (Fig. 7a). These structures form small sedimentary dikes of fine sediment (Demoulin 2003) showing random directions of propagation and suggesting high-energy impact of a landward-directed sediment surge.

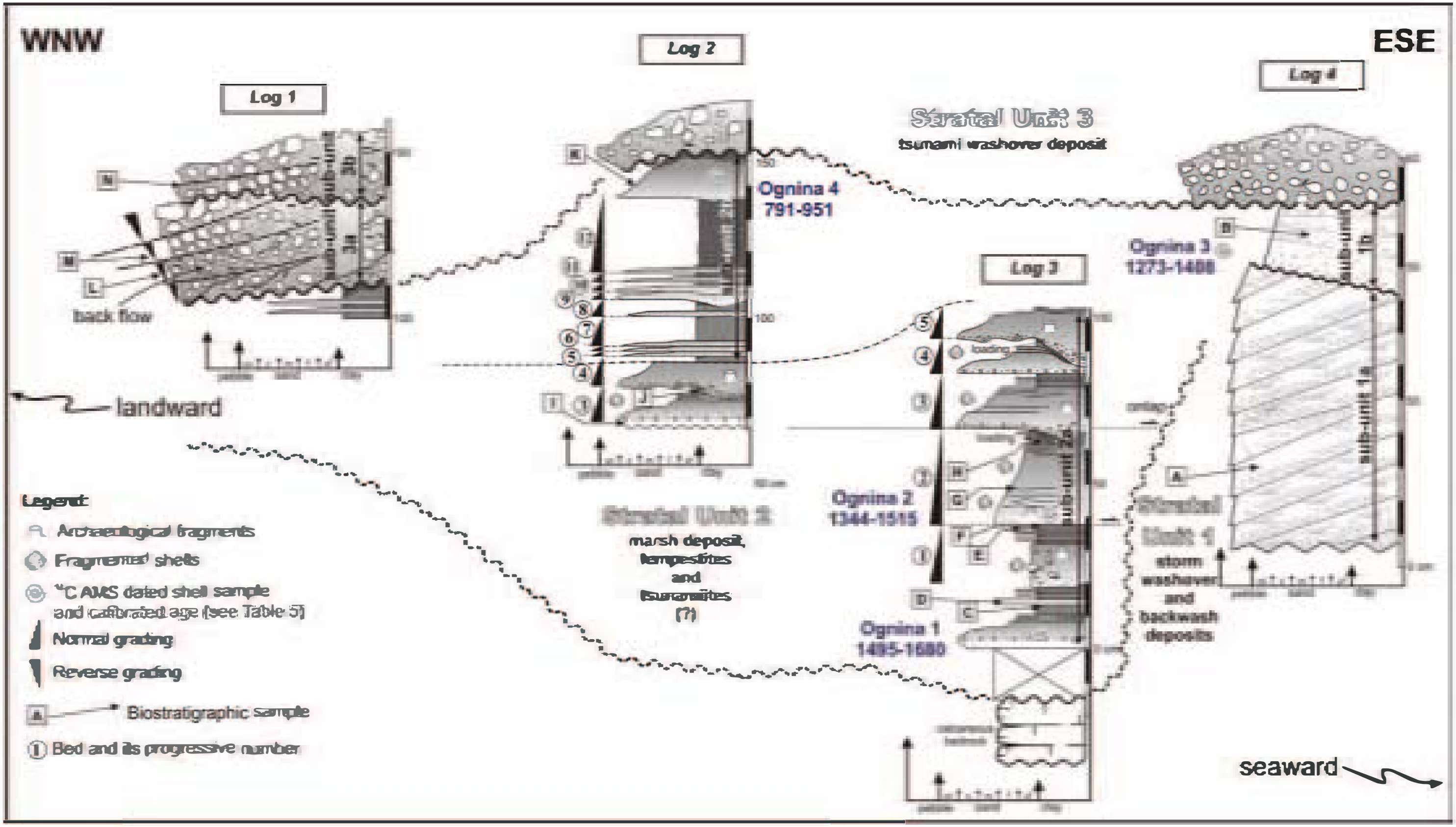

Fig. 5. Sedimentological logs measured across the study succession showing its sub-division into stratal units and sub-units (see Fig. 2e for location). Numbers indicate the studied intervals within marsh deposits. Letters indicate biostratigraphic samples. Samples for radiocarbon and archaeological dating are also indicated.

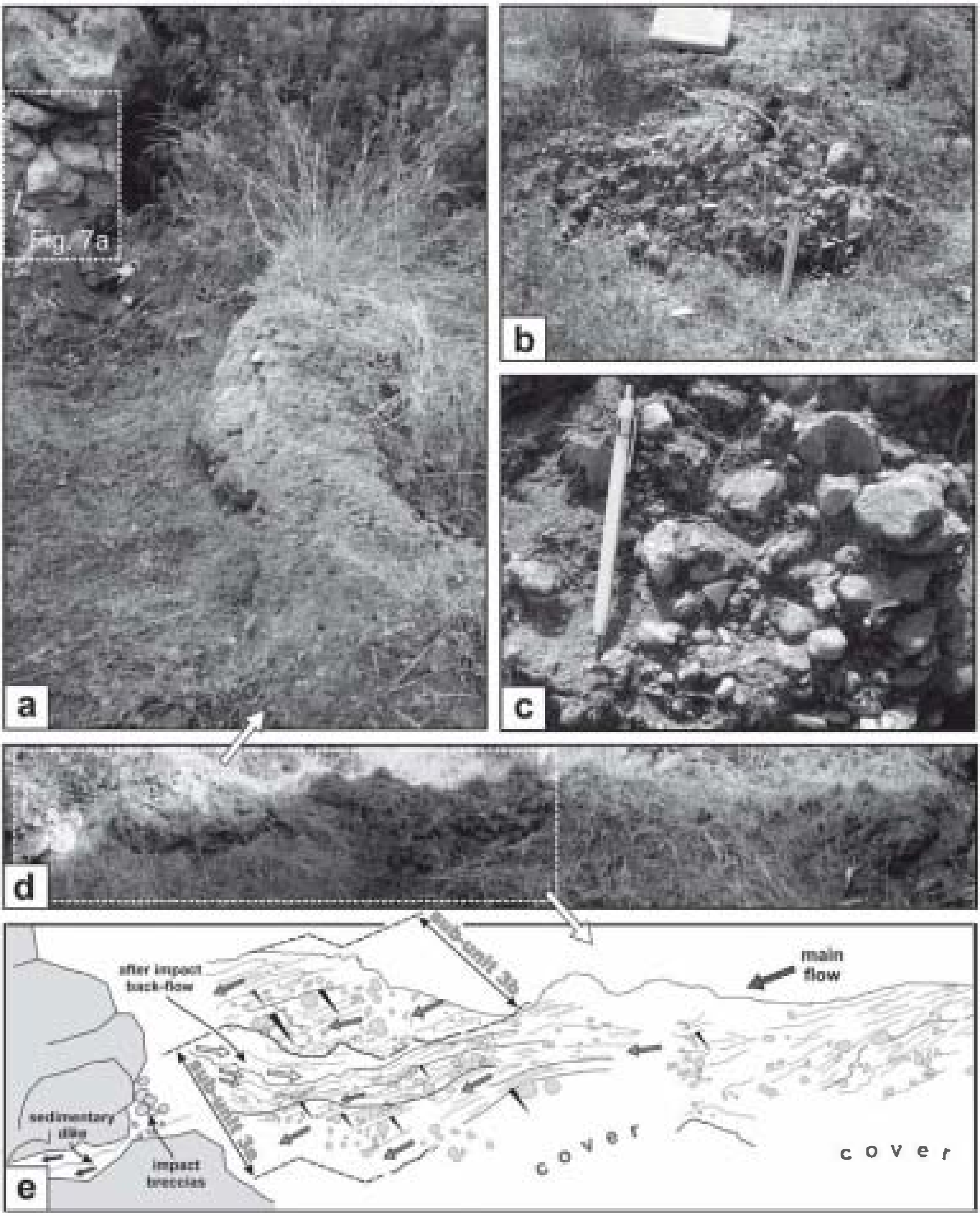

Fig. 7a
a
b
c
d
after impact back-flow
main flow
sedimentary dike
impact breccias
cover
cover
e

Fig. 6. (a) Inland termination of the study section occupied by Stratal Unit 3 (see Fig. 2e for location); the unit is incised by present-day ephemeral streams, the calcareous bedrock in the background. (b, c) Details of the outer segment (seawards) of Stratal Unit 3. This unit shows here the minimum thickness and overall chaotic assemblage with unsorted, sub-angular clasts. (d) On the contrary, the inner (landwards) segment of Stratal Unit 3 is organized into two sub-units, probably related to two successive depositional events. (e) The lower sub-unit 3a shows reverse-graded beds (black arrows) and landward-dipping foresets (grey arrows). In the inner part, this sub-unit exhibits a foreset with seaward dipping-laminae (white arrows), probably induced by after-impact back-flow. The upper sub-unit 3h truncates the underlying sub-unit and records the inferred total run-up of the marine flooding. Note the occurrence of calcareous breccias as result of violent mechanical rock fragmentation and high-pressure sedimentary dikes.

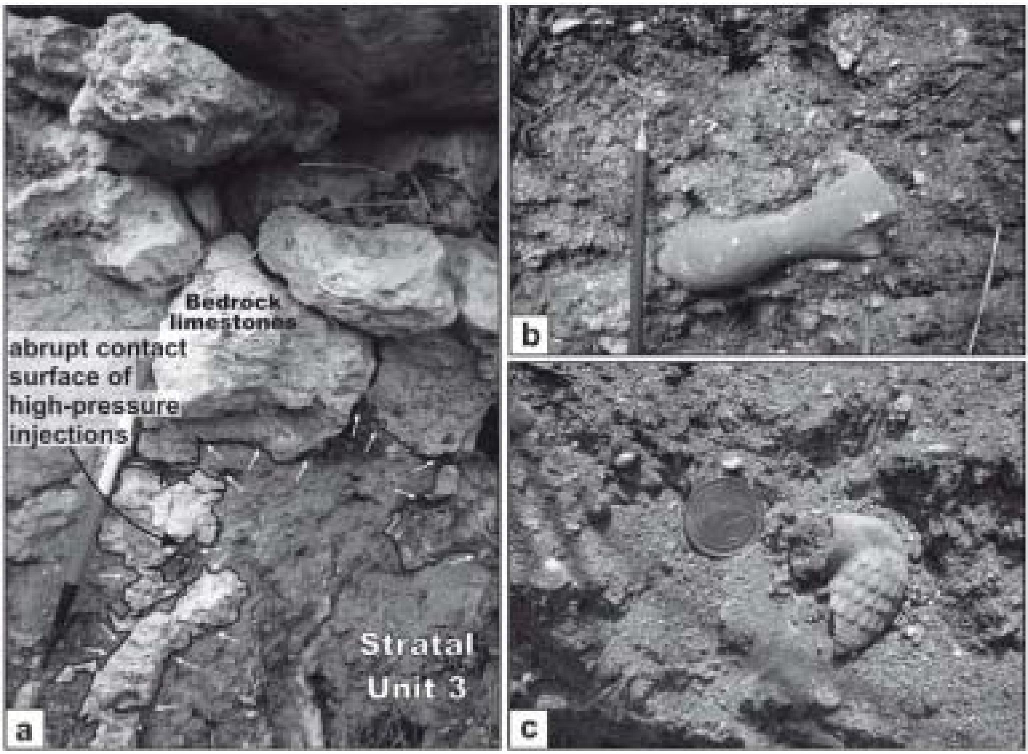

Fig. 7. (a) Detail of the calcareous bedrock at the innermost termination of Stratal Unit 3 (see Fig. 6a for location). Note red-coloured sedimentary dikes filling pre-existing fractures, organized in centrifugal directions (white arrows). (b, c) Archaeological fragments within Stratal Unit 3.

Mollusc assemblage (Table 3) is mainly represented by marine species of *Posidonia* meadows (HP) and photophylic algae (AP) biocenosis, with abbundant Rissoidae and Trochidae; *Cerithium vulgatum* and *Bittium reticulatum* are also well represented. Lagoon species are less frequent or very scarce. Fragments of bivalves living in the sublittoral zone, such as *Pinna nobilis* and *Ostrea* sp., have been found in the coarser fraction. The foraminifer content (Table 4) is similar to that described for Stratal Unit 2. It's noteworthy the bad degree of preservation especially of the marine species and the high percentage of mollusc fragments. Reworked forams are very abundant as well.

Sediment of Stratal Unit 3 is also characterized by the occurrence of abundant fragments of human manufactures, often incrusted by serpulids (Figs. 7b and 7c).

3.3 *Absolute and archaeological dating*

Archaeological determinations have been performed in order to obtain chronological constraints for the studied deposits, useful in the attempt of reconstructing the depositional evolution of the area. Pottery and glass fragments have been found at distinct levels in the Stratal Units 1 and 2 (Fig. 5). The archaeological age determination allowed us to attribute these sequences to the Late Roman-Middle Age period (IV–XII century). As regards the Stratal Unit 3, several earthenware fragments are dispersed in the chaotic deposit. Some of these (e.g., the well preserved pipe in Fig. 7c) have been attributed to XVII–XVIII century, whereas no younger human manufactures have been found. This allowed us to well constrain the age of the upper unit that should have deposited at the passage between the XVII and XVIII centuries.

Radiocarbon age determinations have allowed us to better constrain the dating of the Stratal Units 1 and 2 (Table 5). The results of the AMS analyses have been calibrated by using the CALIB 5.0 software (Stuiver & Reimer 1993; Stuiver et al. 2005) whose marine calibration incorporates a time-dependent global ocean reservoir correction of about 400 years. ^{14}C AMS determination for *Cerastoderma* sp. shells collected from the base, the lower and the upper part of Stratal Unit 2 (see Fig. 5 for location) yielded calendar ages of

Table 5. 14C AMS dating results from shells collected in the Ognina outcrop (see fig. 5 for location) and analyzed at the Poznan Laboratory (Poland). All samples were calibrated using the program Calib 5 (Stuiver & Reimer, 1993; Stuiver et al. 2005) whose marine calibration incorporates a time-dependent global ocean reservoir correction of about 400 years.

Sample Number	Laboratory number	Fossil species	Stratal unit	^{14}C Age [yr BP]	Calibrated Age [cal yr BP 2σ]
Ognina 4	Poz-17756	*Cerastoderma* sp.	2 (sub-unit 2b)	1340 ± 30	791-951
Ognina 3	Poz-25141	*Cerithium sp.*	1 (sub-unit 1b)	1800 ± 30	1273-1408
Ognina 2	Poz-20537	*Cerastoderma* sp.	2 (sub-unit 2a)	1885 ± 30	1344-1515
Ognina 1	Poz-20404	*Cerastoderma* sp.	2 (sub-unit 2a)	2010 ± 30	1495-1680

1495–1680 yr BP, 1344–1515 yr BP and 791–951 yr BP, respectively (Table 5), confirming the archaeological attribution of Stratal Unit 2 to the Late-Ancient age. Furthermore, ^{14}C AMS result from *Cerithium* sp. shell sampled in the upper portion of Stratal Unit 1 (Sub-unit 1b) yielded calendar ages of 1273–1408 yr BP. These radiocarbon ages suggest that deposition of the Stratal Units 1 and 2 was partially coeval.

3.4 *Environmental interpretation*

The interpretation of the three stratal units detected within the Ognina section is strictly related to their sediment composition and physical properties, such as sediment grain size and sorting, degree of internal organization, nature of bounding surfaces, fossil content and relative position along an original depositional profile (Fig. 5). All these features, supported by radiometric and archaeological dating, have allowed us to reconstruct the timing and the modality of depositional processes setup (e.g. flow energy, sediment deliver) and the influence exerted by the original setting on the depositional environments.

Stratal Unit 1 occupies the outermost position along the bay (seawards) and consists of two sub-units, 1a and 1b (Fig. 3a). The observed textural features and depositional architectures are very similar to those described by Schwartz (1982), Foster et al. (1991) and Tuttle et al. (2004) for wash-over coastal deposits (e.g. Switzer et al. 2006; Kortekaas & Dawson 2007; Morton et al. 2008b). In detail, internal organization of the lowermost sub-unit 1a suggests the influence of a series of landward-directed pulsatory flows, producing uninterrupted avalanching of well-sorted sandy sediments and the consequent formation of foresets. The abundance of shell fragments organized into packages of foresets (Fig. 3b), indicates that the flows were generated by waves shoaling along a shallow water shoreface. The occurrence of scattered pebbles suggests that the flows reached picks of energy during the most vigorous events. Repeated wave-driven flows produced a beach-barrier system, isolating the innermost sector and favoring the deposition of Stratal Unit 2. Fossil content, represented by shallow water marine forms, also confirm a beach environment strongly influenced by wave motion, during sediment accretion. Unbroken shells organized into packages of foreset laminae imply that their emplacement mechanism developed over a long period (from days to weeks), excluding instantaneous and catastrophic deposition of mass flows. In contrast, the upper sub-unit 1b, characterized by a better sorting of sediment organized into seaward gently dipping laminae, is typical of beach swash zone (foreshore *sensu* Walker & Plint 1992). This subunit probably represents the consequent backwash and re-establishment of low-energy (fair-weather) beach conditions after a period of reiterated marine storms. Accordingly, the whole Stratal Unit 1 can be interpreted as a sandy supratidal bar, built under the initial action of pulsatory wave-induced flows, forming a small beach-barrier system located in the innermost part of the narrow rocky embayment (Fig. 8).

Stratal Unit 2 occupies an intermediate position along the study section (Fig. 2), onlapping seawards the underlying Unit 1 and landwards the calcareous bedrock. Both sediment grain size and internal organization suggest a low energy environment, where sedimentation of fine particles occurred by settling along a protected water column. The fining-upward

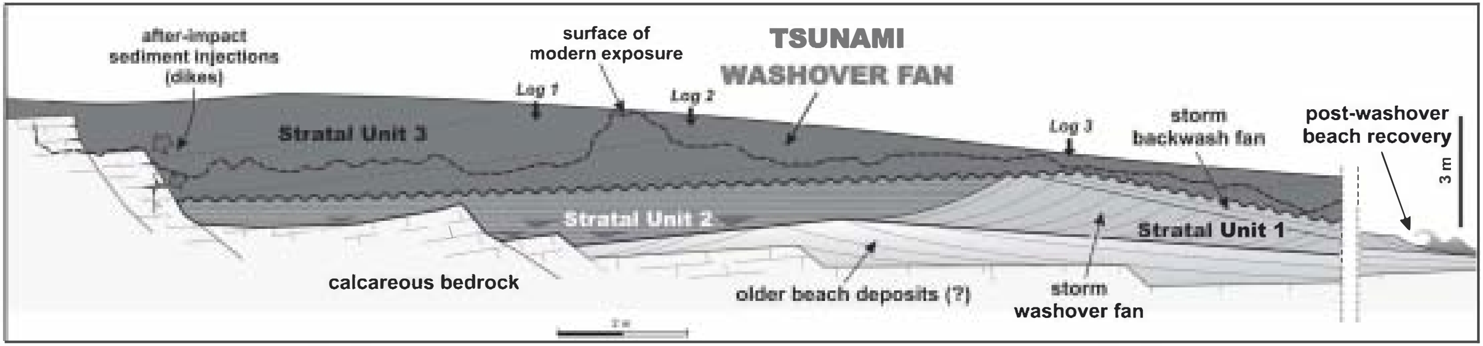

Fig. 8. Inferred depositional 2D model interpreting the Ognina succession. Stratal Unit 1 occupies the outer part of the system forming an original beach-barrier ridge, developing on to pre-existing beach deposits (not exposed in outcrop). This barrier might have favored marsh and lagoonal sedimentation at the shoulder of the system, seasonally reached by high-energy marine events or tsunamis (Stratal Unit 2). The system was suddenly deactivated by the violent deposition of Stratal Unit 3 that, according to our interpretation, represents a tsunami washover fan deposited by a destructive sediment surge caused by a coastal marine flooding.

cycles, observed in the lowermost sub-unit 2a and characterized by erosive basal surfaces and shell/pebble concentrations (Fig. 4b), can be attributed to high-energy, sporadic events that, directed toward the bay and enhanced by the narrowing of the embayment (see Section 4.2), occasionally breached the beach-barrier system flooding a protected lagoonal area (Myrow & Southard 1996; e.g. Kortekaas & Dawson 2007). The cross-laminated silty intervals may represent the effect of inertial tractions deriving from unenergetic flows, whilst the flat-laminated intervals may be related to the re-establish of marsh conditions. These sedimentary structures are absent in the uppermost sub-unit 2b, where the monotonous alternation of thinner clay-rich intervals suggests typical marsh rhythmites (Fig. 4c), regulated by seasonal cyclic little variations of particle grain sizes, from fine sands to clays (Frey & Basan 1985) without any significant high-energy depositional event. The environmental interpretation is also confirmed by the fossil content which is represented by badly preserved shallow marine water association within sub-unit 2a, and by well preserved brackish assemblages within sub-unit 2b.

Stratal Unit 3 shows sedimentary features completely different from the underlying Stratal Units 1 and 2, in terms of sediment grain size, sorting, internal organization and overall geometry. The following points are particularly remarkable:

1) The basal bounding surface irregularly extending over the underlying units shows deep erosion thus suggesting high-energy, very rapid propagation of a landward directed mass surge.

2) The highly variable grain size of clasts indicates high transportation capacity by a non-gravitative mass flow, generating turbulent suspension of different-in-size clastic particles. In a similar coastal setting, this kind of mass flow can be produced by violent and sudden dynamic events, as marine storms, hurricanes or tsunami waves (Nardin et al. 1979), moving from the sea landward and capable to run up over supralittoral environments. Landward-dipping foresets of sub-unit 3a, which exhibit thinner foresets with opposite (seaward) direction, may generate by the bedrock which acted as an obstacle in the inland propagation of this sediment surge. After a first impact, part of the flow may return back, producing a seaward directed high-energy back-flow.

3) The fossil content, constituted by a chaotic mixture of shallow marine water and by brackish associations, indicate a violent transport and a subsequent sudden deposition.

4) The indistinct bounding surfaces that delimitate landward-dipping strata are interpreted as the result of depositional mechanism occurring simultaneously with the flow inland propagation. Although the deposition might occur very rapidly, the sedimentary building of the deposit might follow a progressive landward shift caused by a progressive energy loss during its translation over the beach- and back-barrier systems. This is also confirmed by a landward slight decrease in the main sediment grain size (e.g. Kortekaas & Dawson 2007; Morton et al. 2007; 2008a).

5) The reverse-grading of clinostrata in the innermost part of Stratal Unit 3 indicates that the flow was subjected to an increase of energy during the depositional event (Hiscott 2003), probably triggered by the narrowing of the embayment. This condition may have produced grain collision in a basal grain-rich layer sheared along by an overriding flow caused by dispersive pressure (Bagnold 1956).
6) Pottery fragments encrusted by *serpulids* scattered within this chaotic deposit also indicate that archaeological rests were transported in to the supratidal zone after a period of permanence in subaqueous conditions.

All these features allowed us to interpret Stratal Unit 3 as the sedimentary record of a sudden and violent mass flow caused by a marine flooding. Furthermore, similar characteristics have been described and have been related to tsunami deposits (e.g. Foster et al. 1991; Dawson 1994; Dawson et al. 1996; Goff et al. 1998; Dawson & Shi 2000; Kortekaas 2002; Switzer et al. 2006; Kortekaas & Dawson 2007; Morton et al. 2008a; 2008b). In particular, Stratal Unit 3 may represent a tsunami washover fan (Fig. 8) caused by a catastrophic wave capable to transport a great amount of debris landwards into a protected back-barrier area. Since the inland termination of the deposits is formed by a rocky wall, it is reliable to suppose that the marine surge could have reached a more inland extension than those effectively occupied by the study deposit. This is confirmed by the occurrence of high-pressure forceful injection structures observed at the bedrock contact (Fig. 7a), probably due to the violent impact of the flow against an obstacle (see Le Roux et al. 2008).

4 *Physical processes of tsunami deposition*

4.1 *Depositional implications*

Stratal Unit 3 records the violent emplacement of a tsunami-driven mass flow on a wave- and storm-influenced beach-barrier system formed by Stratal Units 1 and 2. High-speed and high-concentration sediment mass flows are primarily granular flows (Straub 1996). In nature, some granular flows can be generated by non-gravitative mass processes related to sudden high-energy events, such as violent storms, typhoons, hurricanes or tsunami (Nardin et al. 1979). Some aspects related to mechanic behavior of these flows are quite similar to 'canonically gravitative' mass flows (e.g. Nemec 1990). For what concerns tsunami-driven mass flows, the main transport mechanism is represented by an anomalous marine wave (or a set of shortly outdistanced waves) shoaling landwards and induced by submarine slides, subaerial landslides that enter water bodies and/or offshore earthquakes (e.g. Bryant 2001). As the wave approaches shallow-water environments, a surge formed by marine water, sediment detached from the sea floor and living organism develops. When such a catastrophic flow strikes the coast, it may generate a cohesion-less debris flow containing a variety of grain size ranging from silt to boulders (Dawson & Shi 2000), whose propagation momentary prevails on to the gravity force. When a high-energy state of stress is applied to a rapidly moving flow a shear-strain rate may occur, producing violent impacts between particles along a slip surface involving the entire mass of sediment; consequently, this condition can be considered as developing in a *rapid-flow regime* (Savage 1983; Campbell & Brennen 1983; Straub 1996). The process of grain dispersion within a rapidly-moving surge may be pervasive with momentary contact between particles that move in a quasi-random manner (granular flows at the microstructural level are governed by deterministic chaos; Straub 1996) about the average motion vector of the shearing sediment mass (Campbell 2002; 2005). This condition might have occurred during the deposition of Stratal Unit 3 at the scale of each single clinostratum. Their deposition may reflect repeated, quasi-instantaneous stages of sediment accumulation due to violent pulsatory surges. Hypothetically, if the energy of a debris flow is particularly high, the consequent sediment assemblage may occur without the formation of significant depositional structures. On the contrary, if sediment deposition occurs after a partial dissipation of its original energy, sediment may be deposited under a certain degree of internal organization and foreset strata may form, each characterized by reverse-graded of clasts indicating high-energy particle dispersions during deposition (Nemec 1990).

In our case, the deposition of Stratal Unit 3 might reflect this condition of 'energy dissipation'. Such condition may have occurred during the tsunami wave inland translation against an obstacle represented by the ridge of the Ognina beach-barrier system.

The internal organization of Stratal Unit 3 into two sub-units, each composed by clinostrata may suggest that the tsunami event probably was not represented by a single wave, but by a sequence of anomalous waves that stroke the coast during a short time interval. The tsunami deposition might take place within a restricted sector, bounded by a rocky internal seawall that violently stopped the initial flow inland propagation producing energy dissipation. This process may explain the occurrence of calcareous breccias at the top of the bedrock, as consequence of mechanic rock fragmentation after the impact, and the seaward-dipping lamination observed within the sub-unit 3a, as consequence of a post-impact backflow (Fig. 6e). This latter feature is absent within the sub-unit 3b, because the tsunami flood level (run up) might have been higher than the elevation of the internal rocky wall of the channel, so that no obstacles might exist during this second phase of inundation and consequent sediment deposition.

4.2 *Morphological implications*

The elements that concur to better distinguish storm from tsunami provenance of coastal deposits were critically discussed by Nanayama et al. (2000), Kortekaas & Dawson (2007; Tab. 1, p. 209) and Morton et al. (2008b) among others. Tsunami deposits differ from storm-deposited sediments for a series of physical attributes, coinciding or not, such as overall morphologies and stratigraphic architecture of the deposits, sedimentological features, geochemical and palaeontological evidences. In particular, storm washover fans preserved behind breached barriers are thinning inland and of relative smaller extent, consist of better sorted, fining-upward sediments and contain well-preserved fossils of shallow-water provenance (Schwartz 1982; Noe-Nygaard & Surlyk 1988). In contrast, tsunami washover fans recognized within similar depositional settings, show a thickening-inland larger extent (e.g. Dawson & Stewart 2007), unsorted chaotic sediments (e.g. Morton et al. 2008a) and a mixture of poorly-preserved, marine and brackish water fossils (e.g. Morton et al. 2007; see also Vött et al. 2006, 2009).

In order to justify the modality of emplacement of coarse deposits of Ognina section, we retain strategic to analyze the physiography of the Ognina area, as it may have played a fundamental role in the depositional processes and sediment accumulation. The Ognina embayment is a narrow V-shaped channel incised along a rocky coast that has not undergone substantial morphological variations during last hundreds of years. Beach-barrier systems are largely diffused along the central Mediterranean coasts but rarely do they develop within quasi-confined embayments of rocky shorelines. This kind of morphological setting presently occurs along the Pacific coast of the Japan, recently subjected to the effects of catastrophic tsunami waves (Nakao 2007). Accordingly, on June 15, 1896, a huge tsunami wave struck the Sanriku coast of the Tohoku region, characterized by *ria*-type morphology. This anomalous wave shoaled inside some of the narrow embayments along the rocky coast and underwent hydraulic amplification. In this setting, the drastic reduction of the hydraulic cross-section during the wave propagation induced a rapid increasing in the flow velocity and wave height also caused by the drastic landward reduction of bottom depth. Such a circumstance can be applied also to stormy, high-energy waves that seasonally characterize the Ionian coast of Sicily. Their effect, in terms of sedimentary record, is "normal" along a rectilinear coast, but can be considered "anomalous" along complex rocky coast, as *rias* or embayments, subjected to hydraulic amplification. For these reasons, it is often difficult to distinguish storm from tsunami-generated deposits and this is a large debated issue especially in the very recent scientific literature (e.g. Kortekaas & Dawson 2007; Morton et al. 2007; Bridge, 2008 and reply by Jaffe et al. 2008; Morton et al. 2008b; Switzer & Jones 2008).

Another indication of tsunami wave transport can be represented by several archaeological ceramic fragments, encrusted by marine organisms, scattered in chaotic deposits. In the Ognina section, this feature has been observed in the Stratal Unit 3 even though some coarse levels of Stratal Unit 2 contain small pottery and glass fragments. In conclusion, if the uppermost Stratal Unit 3 can be unquestionably referred to a catastrophic tsunami event, the coarser deposits occurring within Stratal Unit 2 can be attributed to high energy marine floods that were capable to reach protected coastal environments as back-barrier marsh or lagoons, and that can be interpreted either as amplified marine storm waves or as lower-energy tsunami events.

5 *Conclusions*

Beach-barrier systems are largely diffused along the central Mediterranean coasts but rarely they develop in quasi-confined embayments along rocky shorelines. The Ognina section represents one of these unusual settings, where landward-shoaling waves can be subjected to hydraulic amplification and their effects into the beach can simulate destructive events. Accordingly, distinction between storm and tsunami deposits has to be afforded using multidisciplinary approaches (e.g. Tappin 2007; Kortekaas & Dawson 2007; Dawson & Stewart 2007).

Our cross-checked analyses allowed us to interpret the three stratal units forming the Ognina section as follow (Fig. 8): the internal architecture of the well-sorted sediments forming the Stratal Unit 1 suggests that it might derive by the superimposition of a landward-directed washover fan (lower sub-unit 1a) and a seaward-directed small backwash fan (upper sub-unit 1b), whose emplacement we attribute to the depositional effect of a series of repeated storm surges of weekly/monthly duration and successive seaward beach recovery. Radiocarbon age of shells collected from Stratal Units 1 and 2 suggest that deposition of these units was partially coeval. The growth of Stratal Unit 1 produced, in fact, morphological confinement for the subsequent beach-barrier development. The isolation from the sea favored marsh sedimentation in the inner part of the system, seasonally reached by high-energy waves of short duration, and responsible of the deposition, within the marsh laminites, of the coarser lenticular layers containing a mixture of shallow-marine and brackish-water fauna associations (Stratal Unit 2). Radiocarbon dating of bivalve shells constrains the age of the lowermost Stratal Unit 2 (sub-unit 2a) to the IV century, whereas its top can be younger than the XII century. Moreover, several pottery and glass fragments of Late-Ancient age have been found at distinct levels in the bioclastic lenses. Taking into account the historical seismicity of south-eastern Sicily and the physiographic setting of the Ognina embayment, amplified marine storm waves or lower energy tsunami events could have been responsible for the deposition of some of the coarser intervals observed within the sub-unit 2a, which are absent in the uppermost part of Stratal Unit 2. This depositional system was dramatically deactivated after the emplacement of the chaotic deposit of the Stratal Unit 3, probably occurred between the XVII and the XVIII century.

Textural and grain size characters of Stratal Unit 3, together with the overall internal architecture and paleontological and archaeological contents, indicate unequivocally the derivation from a destructive, high-energy and landward-directed surge of a non-gravitative mass flow. This chaotic material was instantaneously detached, transported and deposited by an anomalous wave that after having crossed the entire embayment and jumped over the barrier of Unit 1, erosively reached and filled the repaired lagoon. The whole features suggest that a tsunami wave would have been responsible for the deposition of this unit, as most characters are incompatible with the depositional regime of a beach-barrier environment. The catastrophic wave was subjected to hydraulic amplification due to the progressive inland narrowing of the gulf, which produced a series of high-energy sediment surges.

Taking into account the high density of population living on the coastal plains of eastern Sicily, tsunamis represent one of the major factors of geological risk. Ancient chronicles report that the Ionian coast of Sicily was struck by large tsunamis in historical times. In order to relate some of the Ognina stratal units to tsunami events occurred in the Siracusa area, archaeological determinations and radiocarbon dating on marine organisms were compared to the most complete and updated tsunami catalogues for the Mediterranean area (see Soloviev et al. 2000; Tinti et al. 2004). In the last 2,000 years several seismic events, most of which with local sources, could have triggered tsunami waves associated with the coarse deposits occurring in the Ognina succession.

Although sedimentary features of the coarser layers of Stratal Unit 2 cannot be univocally interpreted, we cannot exclude that some of these horizons could have been deposited by anomalous waves. Radiocarbon dating suggest that the bottom and top coarse levels of the Stratal Unit 2 could have been triggered by the 365 AD earthquake, which struck the entire eastern Mediterranean coasts, and by the seismic event of February 4, 1169, which destroyed south-eastern Sicily, respectively. Stratal Unit 3, which closes the entire succession, can be very likely related to the large tsunami of January 11, 1693. Further dating is still in progress in order to better constrain the age of the remaining coarser intervals.

In conclusion, this study represents an useful tool to relate sediment features, coastal morphology and tsunami dynamics, and to revise other coastal deposits occupying similar depositional setting in the Mediterranean area.

Acknowledgements

Many thanks are due to Ernesto De Miro, Elena Flavia Castagnino Berlinghieri and Giuseppe Cacciaguerra for the determination of archaeological fragments, to Cecilia Spampinato for help in preparing samples for paleontological analyses and to Luca Maria Foresi for the precious help in the foraminifer determination. Authors are grateful to the referees Javier Lario and Klaus Reicherter for their useful criticisms.

References

A.A.V.V. (1987): Carta Geologica della Sicilia sud-orientale. – S.El.Ca., Firenze.

Anderson, H. & Jackson, J. (1987): The deep seismicity of the Tyrrhenian Sea. – Geophys. J. Royal Astr. Soc. **91:** 613–637.

Argnani, A. & Bonazzi, C. (2005): Malta Escarpment fault zone offshore eastern Sicily: Pliocene-Quaternary tectonic evolution based on new multichannel seismic data. – Tectonics **24:** TC 4009, doi: 10.1029/2004TC001656.

Bagnold, R.A. (1956): The flow cohesionless grains in fluids. – Phil. Trans. Soc. London. Ser. A **249:** 235–297.

Baratta, M. (1901): I terremoti d'Italia. – Arnaldo Forni, Bologna.

Bianca, M., Monaco, C., Tortorici, L. & Cernobori, L. (1999): Quaternary normal faulting in southeastern Sicily (Italy): a seismic source for the 1693 large earthquake. – Geophys. J. Int. **139:** 370–394.

Boschi, E., Ferrari, G., Gasperini, P., Guidoboni, E., Smriglio, G. & Valensise, G. (1995): Catalogo dei forti terremoti in Italia dal 461 a.D. al 1980. – Ist. Naz. Geofis., S.G.A., Roma.

Bridge, J.S. (2008): Discussion of articles in "Sedimentary features of tsunami deposits". – Sedimentary Geology **211:** 94.

Bryant, E.A. (2001): Tsunami. The Underrated Hazard. – 320 pp.; Cambridge University Press, Cambridge.

Campbell, C.S. (2002): Granular shear flows at the elastic limit. – J. Fluid Mechanics **465:** 261–291.

Campbell, C.S. (2005): Stress-controlled elastic granular shear flows. – J. Fluid Mechanics **539:** 273–297.

Campbell, C.S. & Brennen, C.E. (1983): Computer simulation of shear flows of granular material. – In: Jenkins, J.T. & Satake, M. (eds.): Mechanics of Granular Materials: New Models and Constitutive Relations: 313–326; Elsevier Science, Amsterdam.

Cello, G., Guerra, I., Tortorici, L., Turco, E. & Scarpa, R. (1982): Geometry of the neotectonic stress field in southern Italy: geological and seismological evidence. – J. Struct. Geol. **4:** 385–393.

CMT Catalogue (1976–2006): http://www.seismology.harvard.edu/CMTsearch.html

D'Agostino N. & Selvaggi G. (2004): Crustal motion along the Eurasia-Nubia plate boundary in the Calabrian Arc and Sicily and active estension in the Messina Straits from GPS measurements. – J. Geophys. Res. **109:** B11402.

Dawson, A.G. & Stewart, I. (2007): Tsunami deposits in the geological record. – Sedimentary Geol. **200:** 166–183.

Dawson, A.G. (1994): Geomorphological processes associated with tsunami run-up and backwash. – Geomorphology **10:** 83–94.

Dawson, A.G. & Shi, S. (2000): Tsunami deposits. – Pure and Appl. Geophys. **157:** 875–897.

Dawson, S., Smith, D.E., Ruffman, A. & Shi, S. (1996): The diatom biostratigraphy of tsunami sediments: examples from Recent and Middle Holocene events. – Phys. and Chem. Earth **21:** 87–92.

Demoulin, A. (2003): Clastic (Neptunian) dikes and fills. – In: Middleton, G.V. (ed.): Encycl. Sediments and Sedimentary Rocks: 136–138; Springer.

Ferranti, L., Monaco, C., Antonioli, F., Maschio, L., Kershaw, S. & Verrubbi, V. (2007): The contribution of regional uplift and coseismic slip to the vertical crustal motion in the Messina Straits, Southern Italy: evidence from raised Late Holocene shorelines. – J. Geophys. Res. **112:** B06401, doi: 10.1029/2006JB004473.

Foster, I.D.L., Albon, A.J., Bardell, K.M., Fletcher, J.L., Jardine, T.C., Mothers, R.J., Pritchard, M.A. & Turner, S.A. (1991): High energy coastal sedimentary deposits; an evaluation of depositional processes in southwest England. – Earth Surf. Proc. and Landf. **16:** 341–356.

Frey, R.W. & Basan, P.B. (1985): Coastal salt marshes. – In: Davis, R.A. Jr. (ed.): Coastal Sedimentary Environ.: 225–289; Springer-Verlag.

Gasparini, C., Iannacone, G., Scandone, P. & Scarpa, R. (1982): Seismotectonics of the Calabrian Arc. – Tectonophysics **82:** 267–286.

Goff, J.R., Crozier, M., Sutherland, V., Cochran, U. & Shane, P. (1998): Possible tsunami deposit from the 1855 earthquake, North Island, New Zealand. – In: Stewart, I.S. & Vita-Finzi, C. (eds.): Coastal Tectonics. – Geol. Soc., London, Spec. Publ. **146:** 353–374.

Hiscott, R.N. (2003): Grading, graded bedding. – In: Middleton, G.V. (ed.): Encycl. Sediments and Sedimentary Rocks: 333–335; Springer.

Jacques, E., Monaco, C., Tapponnier, P., Tortorici, L. & Winter, T. (2001): Faulting and earthquake triggering during the 1783 Calabria seismic sequence. – Geophys. J. Int. **147:** 499–516.

Jaffe, B.E., Morton, R.A, Kortekaas, S., Dawson, A.G., Smith, D.E., Gelfenbaum, G., Foster, I.D.L., Long, D. & Shi, S. (2008): Reply to Bridge (2008): Discussion of articles in "Sedimentary features of tsunami deposits". – Sedimentary Geol. **211:** 95–97.

Kortekaas, S. (2002): Tsunamis, storms and earthquakes: distinguishing coastal flooding events. – PhD-thesis: 171 pp.; Coventry University, UK.

Kortekaas S. & Dawson, A.G. (2007): Distinguishing tsunami and storm deposits: an example from Martinhal, SW Portugal. – Sedimentary Geol. **200:** 208–221.

Le Roux, J.P., Nielsen, S.N., Kemnitz, H. & Henriquez, A. (2008): A Pliocene mega-tsunami deposit and associated features in the Ranquil Formation, southern Chile. – Sedimentary Geol. **203:** 164–180.

Makris, J., Nicolich, R. & Weigel, W. (1986): A seismic study in the western Ionian Sea. – Ann. Geophys. **6:** 665–678.

Monaco, C., Tapponier, P. Tortorici, L. & Gillot, P.Y. (1997): Late Quaternary slip rates on the Acireale-Piedimonte normal faults and tectonic origin of Mt. Etna (Sicily). – Earth Planet. Sci. Lett. **147:** 125–139.

Monaco, C. & Tortorici, L. (2000): Active faulting in the Calabrian arc and eastern Sicily. – J. Geodynam. **29:** 407–424.

Monaco, C. & Tortorici, L. (2007): Active faulting and related tsunami in eastern Sicily and south-western Calabria. – Boll. Geofis. Teo. e Appl. **48** (1): 163–184.

Morton, R.A, Gelfenbaum, G. & Jaffe, B.E. (2007): Physical criteria for distinguishing sandy tsunami and storm deposits using modern examples. – Sedimentary Geol. **200:** 184–207.

Morton, R.A., Goff, J.R. & Nichol, S.L. (2008a): Hydrodynamic implications of textural trends in sand deposits of the 2004 tsunami in Sri Lanka. – Sedimentary Geol. **207:** 56–64.

Morton, R.A., Richmond, B.M., Jaffe, B.E. & Gelfenbaum, G. (2008b): Coarse clast coastal ridges of the Caribbean region: a re-evaluation of processes and origins. – J. Sedimentary Res. **78:** 624–637.

Myrow, P.M. & Southard, J.B. (1996): Tempestite deposition. – J. Sedimentary Res. **66:** 875–887.

Nakao, M. (2007): The great Meiji Sanriku tsunami. – Failure knowledge database; http://shippai.jst.go.jp/en/Search.

Nanayama, F., Shigeno, K., Satake, K., Shimokawa, K., Koitabashi, S., Miyasaka, S. & Ishii, M. (2000): Sedimentary differences between the 1993 Hokkaido-nansei-oki tsunami and the 1959 Miyakojima typhoon at Taisei, southwestern Hokkaido, northern Japan. – Sedimentary Geol. **135:** 255–264.

Nardin, T.R., Hein, F.J., Gorsline, D.S. & Edwards, B.D. (1979): A review of mass movement processes, sediment and acoustic characteristics, and contrasts in slope and base-of-slope systems versus canyon-fan-basin floor systems. – In: Doyle, L.J. & Pilkey. O.H. (eds.): Geology of Continental Slopes. Soc. Econ. Paleontol. Mineral. Spec. Pub. **27:** 61–73.

Nemec, W. (1990): Aspects of sediment movement on steep delta slopes. – In: Colella, A. & Prior, D.B. (eds.): Coarse-grained deltas. – International Association of Sedimentologists Special Publication **10:** 29–73.

Noe-Nygaard, N. & Surlyk, F. (1988): Washover fan and brackish bay sedimentation in the Berriasian-Valanginian of Bornholm, Denmark. – Sedimentology **35:** 197–217.

Pérès, J.M. (1967): The Mediterranean benthos. – Oceanogr. Mar. Biol. Ann. Rev. **5:** 449–533.

Pérès, J.M. & Picard, J. (1964): Noveau manuel de bionomie benthique de la Mer Méditerranée. – Rec. Trav. Stat. Mar. Endoume **47** (31): 137 pp.

Postpischl, D. (1985): Catalogo dei terremoti italiani dall'anno **1000** al 1980. – 239 pp.; CNR, P.F. Geodinamica, Graficoop, Bologna.

RCMT Catalogue (1997–2006): http://mednet.ingv.it/events/QRCMT/Welcome.html

Sabelli, B., Savelli, G.R. & Bedulli, D. (1992): Annotated Check-List of Mediterranean Marine Mollusks. – Soc. Ital. Malacol. **1, 2, 3**: 1–781.

Sartori, R., Colalongo, M.L., Gabbianelli, G., Bonazzi, C., Carbone, S., Curzi, P.V., Evangelisti, D., Grasso, M., Lentini, F., Rossi, S. & Selli, L. (1991): Note stratigrafiche e tettoniche sul rise di Messina (Ionio nord-occidentale) – G. Geol. **53:** 49–64.

Savage, J.F. (1983): Statistics of slide blocks. – J. Struct. Geol. **5:** 627–628.

Scandone, P., Patacca, E., Radoicic, R., Ryan, W.B.F., Cita, M.B., Rawson, M., Chezar, H., Miller, E., Mckenzie, J. & Rossi, S. (1981): Mesozoic and Cenozoic rocks from Malta Escarpment (Central Mediterranean). – A.A.P.G. Bull. **65:** 1299–1319.

Schwartz, D.E. (1982): Bedform and stratification characteristics of some modern small-scale washover sand bodies. – Sedimentology **29:** 835–849.

Scicchitano, G., Monaco, C. & Tortorici, L. (2007): Large boulder deposits by tsunami waves along the Ionian coast of south-eastern Sicily. – Marine Geol. **238:** 75–91.

Soloviev, S.L., Solovieva, O.N., Go, C.N., Kim, K.S. & Shchetnikov, N.A. (2000): Tsunamis in the Mediterranean Sea 2000 B.C. – 2000 A.D. – 237 pp.; Kluwer Academic Publishers, Dordrecht.

Straub, S. (1996): Self-organization in the rapid flow of granular material: evidence for a major flow mechanism. – Earth and Environ. Sci. **85** (1): 85–91.

Stuiver, M. & Reimer, P.J. (1993): Extended 14C data base and revised CALIB 3.0 14C age calibration program. – In: Stuiver, M., Long, A. & Kra, R.S. (eds.): Calibration 1993. Radiocarbon **35** (1): 215–230.

Stuiver, M., Reimer, P.J. & Reimer, R. (2005): Radiocarbon calibration, execute version 5.0.2 html. – http://calib.qub.ac.uk/calib.

Switzer, A.D., Bristow, C.S. & Jones, B. (2006): Investigation of large-scale washover of a small barrier system on the southeast Australian coast using ground penetrating radar. – Sedimentary Geol. **183:** 145–156.

Switzer, A.D. & Jones, B.G. (2008): Large-scale washover sedimentation in a freshwater lagoon from the southeast Australian coast: sea-level change, tsunami or exceptionally large storm? – The Holocene, **18** (5): 787–803.

Tappin, D.R. (2007): Sedimentary features of tsunami deposits: their origin, recognition and discrimination: an introduction. – Sedimentary G. **200:** 151–154.

Tinti, S., Maramai, A. & Graziani, L. (2004): The new catalogue of Italian Tsunamis. – Nat. Haz. **33:** 439–465.

Tortorici, L., Monaco, C., Tansi, C. & Cocina, O. (1995): Recent and active tectonics in the Calabrian arc (Southern Italy). – Tectonophysics **243:** 37–55.

Tuttle, M.P., Ruffman, A., Anderson, T. & Jeter, H. (2004) - Distinguishing tsunami from storm deposits in eastern North America: the 1929 Grand Banks tsunami versus the 1991 Halloween storm. – Seismological Res. Lett. **75** (1): 117–131.

Vött, A., May, M., Brückner, H. & Brockmüller, S. (2006): Sedimentary evidence of late Holocene tsunami events near Lefkada Island (NW Greece). – Z. Geomorph. N.F., Suppl. Vol. **146:** 139–172.

Vött, A., Brückner, H., Brockmüller, S., Handl, M., May, S.M., Gaki-Papanastassiou, K., Herd, R., Lang, F., Maroukian, H., Nelle, O. & Papanastassiou, D. (2009): Traces of Holocene tsunamis across the Sound of Lefkada, NW Greece. – Gobal and Planetary Change **66:** 112–128.

Walker, R.G. & Plint, A.G. (1992): Wave and storm-dominated shallow marine systems. – In: Walker, R.G. & James, N.P. (eds.): Facies Models: Response to Sea-Level Change. – 219–238; Geol. Assoc. Canada, St John's, Newfoundland.

Ward, S.N. (1994): Constraints on the seismotectonics of the central Mediterranean from Very Long Baseline Interferometry – Geophys. J. Int. **117:** 441–452.

Addresses of the authors:

Dr. G. Scicchitano, Dr. B. Costa, Dr. A. Di Stefano, Prof. C. Monaco, Dipartimento di Scienze Geologiche, University of Catania, Corso Italia, 55, 95129 Catania, Italy; e-mail: cmonaco@unict.it.
Dr. S. Longhitano, Dipartimento di Scienze Geologiche, University of Basilicata, Campus Universitario di Macchia Romana, 85100 Potenza, Italy.